

Cosmological GRBs: Internal vs. External Shocks

Re’em Sari & Tsvi Piran

Racah Institute for Physics, The Hebrew University, Jerusalem 91904, Israel

11 September 2018

ABSTRACT

Internal (IS) or external (ES) shocks in relativistic expanding shells are currently the best known mechanism for producing GRBs. We calculate the hydrodynamic conditions and the cooling processes in internal shocks, that occur when one layer overtakes another. We compare these conditions with the conditions in external shocks that occur when the shell encounters the ISM. We find that the complicated temporal structure observed in GRBs could be easily explained in IS scenario. Unlike ES, the observed temporal structure simply reflects the temporal behavior of the internal engine that produces the shell. We also find that opacity and in particular the opacity for pair production poses strong constraints on the parameter space and consequently bursts with very narrow peaks are expected to be optically thick and would not contain GeV photons. Finally we find that as in ES synchrotron is the most likely radiation process.

Subject heading: gamma-rays: bursts—hydrodynamics—relativity

1 INTRODUCTION

A cosmological γ -ray burst (GRB) occurs, most likely, when the kinetic energy of a relativistic shell turns into internal energy and cools by non-thermal radiation process. The kinetic energy of the shell can be transformed into internal energy by decelerating onto the ISM (Mészáros & Rees 1992), or by internal shocks in the shell (Rees & Mészáros 1994; Narayan, Paczyński & Piran, 1992).

Sari & Piran (1995, denoted hereafter SP) have discussed the hydrodynamics of the deceleration of the relativistic shell on the ISM and internal shocks. If the shell is thin and its Lorentz factor is low, internal shocks form before a considerable deceleration on the ISM takes place. Provided that the Lorentz factor of the shell is not uniform, with fluctuations of the order of a few, these internal shocks can extract a considerable fraction of the shell’s kinetic energy and produce the observed γ -rays.

The internal shock (IS) scenario has several advantages over the external shock (ES) one. Mészáros and Rees (1994) have pointed out that IS requires, quite generally, a lower Lorentz factor. This allows slightly larger amounts of baryonic load in the fireball and it eases, somewhat, the constraints on the source. We demonstrate in sections II and III that the hydrodynamics of IS also offers a natural explanation to the multiple time scales observed in the temporal profiles of the bursts. Such an explanation is missing in the ES scenario.

The observed spectrum indicates that the source must be optically thin. Two processes are relevant for determining the optical depth: Compton scattering on the shell’s electrons and pair production between the γ -ray photons. The relativistic motion of the shell releases the constraint that

the optical depth poses to cosmological GRB sources. In fact this is the main reason to believe that highly relativistic motion is an essential ingredient of any cosmological GRB model (Goodman, 1986; Paczyński 1986; Krolik and Pier, 1989; Piran, 1996). For the ES scenario in which the kinetic energy is deposited at $\sim 10^{15} - 10^{16}$ cm the optical thinness condition leads to a modest limitation on the Lorentz factor $\gamma \geq 100$ (Fenimore Epstein & Ho, 1993; Woods & Loeb 1995; Piran 1996) which is not a serious restriction. For ES a stronger limit on γ arises from the temporal structure. For internal shocks, in which the energy is deposited around $\sim 10^{12} - 10^{14}$ cm this poses an additional constraint which we examine in section IV. In the IS scenario the minimal Lorentz factor is determined by optical thinness condition. We show (in section IV) that the optical depth to pair production poses, usually a stronger constraint than the optical depth to Compton scattering which Mészáros and Rees (1994) used.

Cooling must be rapid enough to allow for the shortest time scale. In a recent paper, Sari, Narayan and Piran (1996 denoted hereafter SNP) have discussed cooling in the ES scenario. In sections V and VI we generalize this discussion to internal shocks, and we discuss the possible observational differences between cooling in the ES and the IS scenarios.

2 TEMPORAL STRUCTURE

Many bursts display a complicated temporal structure with numerous peaks (see e.g. Fishman and Meegan, 1995). We denote by t_{dur} the total duration of the burst and by δt the typical duration of the individual peaks. Few bursts are smooth with $\delta t \approx t_{dur}$. Most bursts are highly variable with $\delta t \ll \Delta T$. Thus any GRB model must be capable of explaining both time scales, the overall duration, t_{dur} , and the duration of the individual peaks, δt . We review here, briefly,

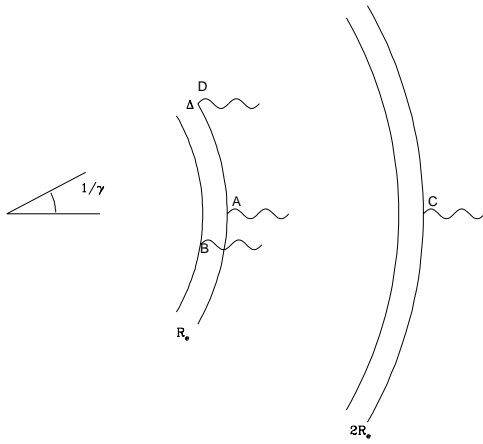


Figure 1. A photon emitted at (A) the outer side of a shell with thickness Δ will reach the observer Δ/c before a photon emitted at the same time (in the observer's frame) from the inner side of the shell (B). A photon emitted at (A) will reach the observer $R_e/2\gamma^2 c$ before a photon emitted by the same electron at $2r_e$ (C). A photon emitted at (A) will reach the observer $R_e/\gamma^2 c$ before a photon emitted by matter that moves radially outwards at an angle $1/\gamma$.

several relativistic effects that determine the temporal structure of the bursts (see Fenimore, Madras and Nayakshin, 1996 for a detailed discussion).

Consider a shell with a width Δ (in the observer frame) and a Lorentz factor γ that converts its kinetic energy to internal energy and cools between R_e and $2R_e$ (see Fig. 1). A photon that is emitted at the outer edge of the shell will reach the observer Δ/c before a photon that is emitted at the same time (in the observer's rest frame) from the inner edge of the shell. Therefore:

$$t_{dur} \geq \Delta/c. \quad (1)$$

We denote by γ_2 the Lorentz factor of the radiating matter (γ_2 is always smaller than γ). A photon that is emitted by a given electron at R_e will arrive $R_e/2\gamma_2^2 c$ before a photon emitted by the same electron at $2R_e$ (the difference arises from the the different time of flight of the photon and the electron from R_e to $2R_e$) (see Fig. 1). Finally the angular width of the observed emitting surface is $1/\gamma_2$ due to relativistic beaming. A photon that is emitted radially outwards will reach the observer $R_e/\gamma_2^2 c$ before a photon that is emitted by matter that moves at an angle $1/\gamma_2$ from the line of sight (Katz, 1994) (see Fig. 1). The last two limits give rise to the same condition, which limits the duration of peaks. If the emission is continuous from R_e to $2R_e$ or if it spreads over a region with an angular width larger than R_e/γ_2 then:

$$\delta t \geq R_e/\gamma_2^2 c. \quad (2)$$

Within the ES scenario there are two possible regimes for deceleration of the shell on the ISM according to the value of the parameter ξ (SP):

$$\xi \equiv (l/\Delta)^{1/2} \gamma^{-4/3}, \quad (3)$$

where $l \equiv (E/n_{ism} m_p c^2)^{1/3}$ is the Sedov length typically $\sim 10^{18}$ cm. If $\xi > 1$ the shock penetrating the shell is only mildly relativistic, the shell decelerates gradually, and $\gamma_2 \cong \gamma$. We call this case the “Newtonian” scenario. If $\xi < 1$ the shell is decelerated by one ultra relativistic shock, which reduces its Lorenz factor from γ directly to $\gamma_2 = \gamma \xi^{3/4}$. This is the relativistic scenario.

In either case the external shock satisfies: $\Delta \leq R_e/\gamma_2^2$. Thus, if the energy conversion in the shell and the subsequent emission is continuous or if the emission spreads over an angular size R_e/γ_2 then $t_{dur} \approx \delta t \approx dt$. This corresponds to a smooth temporal profile with a single peak. Such profiles are observed only in a small minority of the bursts. This conclusion is quite severe. It suggests that angular spreading will smooth all bursts and ES are not capable of producing bursts with complicated time profiles.

A way out of the angular spreading problem, within the external shock scenario, is if the ISM is made out of small dense clouds with a large filling factor. There is an enhanced emission when the shell reaches ISM regions with higher density. This requires large fluctuations in the ISM on the scale of $\approx 10^{12}$ cm (for peaks with $\delta t \approx 0.3$ sec and $\gamma = 100$). Shaviv and Dar (1995, 1996) suggest and explore in details the temporal structure for the scenario in which the shell interacts with a dense population of stars (in a globular cluster or a galactic center) which provide the desired high filling factor. Recently, Li & Fenimore (1996) have found that the distribution of peaks in long GRBs does not correspond to a random distribution. More specifically, the intervals between peaks has a log-normal distribution. Such a distribution is incompatible with a random distribution of objects that the shell encounters. We have already seen that the inner source cannot produce variability on such scale (because of the angular spreading). Hence, this feature, if confirmed, would pose a possible objection to the ES model. *

The essence of the problem in the external shock scenario was the inequality: $\Delta \leq R_e/\gamma_2^2$. We will see shortly that within the IS scenario we have, quite generally, $\Delta > R_e/\gamma_2^2$ and $\gamma_2 \approx \gamma$. Consequently in this case Δ determines the overall duration, t_{dur} , while the angular spreading as well as the radial size of the shell's fluctuations determines the duration of individual peaks, δt . This, in turn, yields some interesting information about the inner source that drives GRBs. It requires that the source produces a shell of relativistic matter of width Δ in which fluctuations of order unity in the Lorentz factor should take place on a scale $\delta \ll \Delta$.

* An alternative solution to the angular spreading problem would be if the source produces an irregular shell composed of many small blobs. Internal pressure will cause any small scale angular structure in the shell to spread radially and tangentially to size R/γ (Narayan and Piran, 1994, Piran 1994). However, recall that $\gamma_2 \ll \gamma$ in the relativistic ES scenario. If the shocked material cools before it expands from R_e/γ to R_e/γ_2 it will produce a short peak on a scale $t_{dur}/c \gamma_2/\gamma$ (Sari and Piran, 1996). Temporal correlation in this substructure could be produced naturally by the internal engine

3 HYDRODYNAMIC OF INTERNAL SHOCKS

Internal shocks occur when the relativistic ejecta from the inner source that drives a GRB is not moving uniformly. If some inner layer moves faster than an outer one it will take over. When the two layers collide two shocks appear - a forward shock propagating into the outer shell and a reverse shock propagating into the inner one. The forward and the reverse shocks have similar conditions behind them since it is most likely that both layers had (prior to the collision) similar conditions. This simplifies the discussion of internal shocks in which the two emitting regions have similar physical condition. In the case of external shocks we had to deal with each shock separately (SNP).

We begin with a short discussion of the hydrodynamics of internal shocks in relativistic shells. Imagine a spherically expanding relativistic shell of thickness Δ in the observer frame moving with a high Lorentz factor γ . Assume further that the Lorentz factor varies by order of a few throughout the shell. Faster shells overtake slower ones. An inner shell will overtake an outer one at a radius, R_s :

$$R_s \sim \delta \gamma^2, \quad (4)$$

where δ is the spatial scale of fluctuations in γ within the shell, and we have ignored factors of order unity. A significant fraction of the kinetic energy is converted to internal energy at this radius.

The observed time over which internal shocks transform the relative kinetic energy of the two colliding layers (whose typical size is $\sim \delta$) is of the order of

$$R_s/\gamma^2 c = \delta/c. \quad (5)$$

This corresponds to a single peak within a burst. Thus it can be identified with the observed quantity δt .

If more than one layer overtakes another one then other regions will collide and other shocks will form. These will be produced in different parts of the shell that are separated by radial distance of Δ . Therefore the total observed duration is given by

$$t_{dur} = \Delta/c. \quad (6)$$

We define the ratio between δ and Δ

$$\zeta \equiv \frac{\delta}{\Delta} \leq 1. \quad (7)$$

Comparison between Eqs. 5, 6 and 7 shows that ζ is also the ratio between the duration of the individual peaks and the overall duration of the burst.

The external shock which is produced by the ISM sweeps the shell by the time it arrives at radius

$$R_\Delta = l^{3/4} \Delta^{1/4}, \quad (8)$$

(see SP). Clearly internal shocks are relevant only if they appear before the external ones. That is only if

$$R_s < R_\Delta. \quad (9)$$

Using Eqs. 4 and 8 condition 9 can be translated to:

$$\xi^{3/2} > \zeta. \quad (10)$$

This generalizes the result of SP who found that $\xi > 1$ (for $\zeta = 1$) is a necessary condition for internal shocks. The condition 10 can be turned into a condition that γ is sufficiently small:

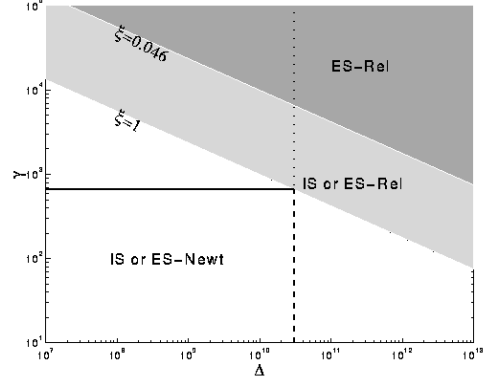


Figure 2. Different scenarios in the Δ ,(in cm) γ plane for $\zeta \equiv \delta/\Delta = 0.01$. Relativistic ES occur for large Δ and large γ - upper right -above the $\xi = 1$ line (dark gray and light gray regions). Newtonian ES occur below $\xi = 1$ - lower left - white region. IS occur, if there are sufficient variation in γ below the $\xi = \zeta^{2/3}$ line (light gray and white regions). The equal duration $t_{dur} = 1$ sec curve is shown for Newtonian ES (solid line) a relativistic ES (dotted line) and IS (dashed line). Note that a relativistic ES and an internal shock with the same parameters have the same overall duration t_{dur} but different temporal substructure depending on δ .

$$\gamma \leq 280 \zeta^{-1/2} \left(\frac{t_{dur}}{10 \text{sec}} \right)^{-3/8} l_{18}^{3/8} \quad (11)$$

We see that internal shocks take place in relatively “low” γ regime. Fig. 2 depicts the regimes in the physical parameter space (Δ, γ) in which different shocks are possible. It also depicts an example of a $t_{dur} = \text{const.}$ line.

Provided that the different parts of the shell have comparable Lorentz factor differing by factor of ~ 2 , the shocks are mildly relativistic. The protons’ thermal Lorentz factor will be of order of unity, and the shocked regions will still move highly relativistically towards the observer with the approximately the initial Lorentz factor γ . Newtonian shocks have a limiting compression of factor of 7 (assuming an adiabatic index of relativistic gas, i.e., 4/3). The density behind the shocks is, therefore, comparable to the density in front of the shocks. In-front of the shocks the particle density of the shell is given by the total number of baryons $E/\gamma m_p c^2$ divided by the co-moving volume of the shell at the radius R_s which is $4\pi R_s^2 \Delta \gamma$. The density behind the shock is higher by a factor of 7.

The hydrodynamical conditions behind the shocks are therefore:

$$n = 7E/4\pi\gamma^6 c^4 m_p t_{dur}^3 \zeta^3, \quad (12)$$

$$e = nm_p c^2 .$$

4 OPACITY CONSTRAINTS

One of the advantages of the internal shock model is that it allows for short bursts with a lower value of the Lorentz factor γ . This eases the baryon purity constraints on source models. However, too low value of the Lorentz factor or too small emission radius could lead to a large optical depth. This poses another limitation on the parameters.

The optical depth for Compton scattering of the photons on the shell's electrons at R_s is given by:

$$\tau_e = (E/\gamma)/(4\pi R_s^2) \sigma_T = 3.9 \times 10^{-5} \zeta^{-2} \times \left(\frac{\gamma}{100} \right)^{-5} \left(\frac{t_{dur}}{100} \right)^{-2} E_{51} . \quad (13)$$

The condition $\tau_e < 1$ yields a lower limit on γ :

$$\gamma \geq 13 \left(\frac{t_{dur}}{10 \text{ sec}} \right)^{-2/5} \zeta^{-2/5} E_{51}^{1/5} , \quad (14)$$

which is not a strong limit.

In addition, the radius of emission should be large enough so that the optical depth for $\gamma\gamma \rightarrow e^+e^-$ will be less than unity ($\tau_{\gamma\gamma} < 1$). There are several ways to consider this constraint. The strongest constraint is obtained if one demands that the optical depth of an observed 100MeV photon will be less than one (Fenimore, Epstein & Ho, 1993 ; Woods & Loeb). Following these calculations and using Eqs. 4 to express R_s we find:

$$\gamma > 100 \left(\frac{\zeta t_{dur}}{100} \right)^{-1/4} \quad (15)$$

Eqs. 11, 14 and 15 constrains γ to a relatively narrow range. In fact the constraint due to $\gamma\gamma$ interaction is always more important than the constraint due to Compton scattering: that is $\tau_{\gamma\gamma} > \tau_e$. In Fig. 3, we plot the allowed regions in the γ and δ parameter space.

Three main conclusions emerge from the discussion so far. First, if the spectrum of the observed photons extends beyond 100MeV (as was the case in the bursts detected by EGRET) and if those high energy photons are emitted in the same region as the low energy ones then the condition on pair production, $\tau_{\gamma\gamma}$, is much stronger than the condition on Compton scattering, τ_e . This increases the required Lorentz factors. In fact even if the spectrum has an upper cutoff of 100MeV then it sets a lower limit of $\gamma \geq 100$. Second, even the Compton scattering limit (which is independent of the observed high energy tail of the spectrum) poses a stronger than expected limit on γ for bursts with very short peaks (see Fig. 3). The Lorentz factor should be as high as 10^3 to yield a peak of 0.3msec. Finally, one sees in Fig. 3 that only in a narrow region in the (δ, γ) plane in which optically thin internal shocks are produced. The region is quite small if the stronger pair production limit holds and in particular there is no single value of γ that can produce peaks over the whole range of observed durations. The allowed region is larger if we use the weaker limits on the opacity. But even with this limit there is no single value of γ that produces peaks with all durations. The IS scenario suggests that bursts with narrow peaks should not have a very high energy tail and that very short bursts should have thermal spectrum.

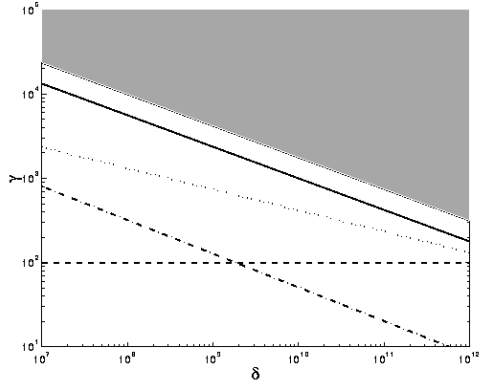


Figure 3. Allowed regions for internal shocks in the δ (in cm), γ plane. Note that the horizontal δ axis also corresponds to δt , the peak duration by a division by c . Internal shocks are impossible in the upper right (light gray) region. The lower boundary of this region depend on $\zeta \equiv \delta/\Delta$ are marked by two solid curves, the lower one for $\zeta = 1$ and the upper one for $\zeta = 0.01$. Also shown are $\tau_{\gamma\gamma} = 1$ for an observed spectrum with no upper bound (dotted line), $\tau_{\gamma\gamma} = 1$ for an observed spectrum with an upper bound of 100MeV (dashed line) and $\tau_e = 1$ (dashed-dotted). The optically thin internal shock region is above the $\tau = 1$ curves and below the $\xi = \zeta^{2/3}$ (solid) lines.

5 SYNCHROTRON COOLING

Following SNP we use the physical conditions derived in the previous section to estimate the cooling of the shocked regions. In order to estimate the radiation processes we need the energy density, e , the particle density, n , given by equation 12 as well as the magnetic field strength, B , and the distribution of electron Lorentz factors γ_e . These last two quantities are difficult to estimate from first principles. Both depend on the microphysics of particle acceleration and magnetohydrodynamics within the shocks. Our approach, following SNP will be to define two parameters, ϵ_B and ϵ_e to incorporate these uncertainties. We then constrain the values of these parameters by requiring the model predictions to resemble the observed features of GRBs.

The dimensionless parameter ϵ_B measures the ratio of the magnetic field energy density to the total thermal energy density, e :

$$\epsilon_B \equiv \frac{U_B}{e} = \frac{B^2}{8\pi e} . \quad (16)$$

Using Eqs. 12 and 16 we can express B in terms of ϵ_B and other observed quantities:

$$B = (720 \text{ G}) \epsilon_B^{1/2} \zeta^{-1} \left(\frac{t_{\text{dur}}}{10 \text{ s}} \right)^{-3/2} E_{51}^{1/2} \left(\frac{\gamma}{100} \right)^{-3}. \quad (17)$$

The second parameter ϵ_e measures the fraction of the total thermal energy e which is in the form of the electrons' random motions:

$$\epsilon_e \equiv \frac{U_e}{e}. \quad (18)$$

Since the electrons obtain their random motions via shock-heating, we make the standard assumption that they develop a power law distribution of Lorentz factors,

$$N(\gamma_e) \sim \gamma_e^{-\bar{\beta}} \quad \text{for } \gamma_e > \gamma_{e,\text{min}}. \quad (19)$$

Following SNP we fix the index $\bar{\beta} \approx -2.5$ and we find that the average electron energy density is

$$\epsilon_e e = 3\gamma_{e,\text{min}} n m_e c^2. \quad (20)$$

Using Eqs. 12 and 20 one finds that the electrons behind the shocks satisfy

$$\gamma_{e,\text{min}} = 610\epsilon_e. \quad (21)$$

The value of $\gamma_{e,\text{min}}$ is sufficient for the calculations of the cooling time scale and efficiency that follow. The exact details of the γ_e distribution are not needed.

We can estimate now the Lorentz factor $\hat{\gamma}_e$, of an electron that is radiating an energy $h\nu \approx 100\text{KeV}$:

$$\hat{\gamma}_e = \left(\frac{m_e c h \nu_{\text{obs}}}{\hbar q_e \gamma B} \right)^{1/2} = 1.1 \times 10^4 \epsilon_B^{-1/4} \zeta^{1/2} \times \left(\frac{h \nu_{\text{obs}}}{100 \text{ KeV}} \right)^{1/2} \left(\frac{t_{\text{dur}}}{10 \text{ s}} \right)^{3/4} E_{51}^{-1/4} \left(\frac{\gamma}{100} \right). \quad (22)$$

We first check that electrons with this Lorentz factor are available. This requires, of course, $\gamma_{\text{min}} < \hat{\gamma}_e$, which corresponds to

$$\epsilon_e < 18\epsilon_b^{-1/4} \zeta^{1/2} \left(\frac{h \nu_{\text{obs}}}{100 \text{ KeV}} \right)^{1/2} \left(\frac{t_{\text{dur}}}{10 \text{ s}} \right)^{3/4} E_{51}^{-1/4} \left(\frac{\gamma}{100} \right). \quad (23)$$

These electrons are always available. A similar situation occurs in a reverse external shock. But in a forward external shock for short burst durations (which force high Lorentz factor) the minimal electron energy is too high and most of the radiation emerges in higher energies than the observed band.

Using the value of $\hat{\gamma}_e$ we can estimate the synchrotron cooling time. The electron's energy divided by the power of its synchrotron radiation (with the appropriate Lorentz transformation from the electron's frame to the observer's frame):

$$t_{\text{syn}} = (0.0014 \text{ sec}) \epsilon_B^{-3/4} \zeta^{3/2} \left(\frac{h \nu_{\text{obs}}}{100 \text{ KeV}} \right)^{-1/2} \times \left(\frac{\gamma}{100} \right)^4 \left(\frac{t_{\text{dur}}}{10 \text{ s}} \right)^{9/4} E_{51}^{-3/4}. \quad (24)$$

This cooling time is shorter than the cooling time estimated for external shocks (SNP) since the magnetic field here is higher. It sets a lower limit to the variability time scale. Clearly, the burst cannot possibly contain spikes that are shorter than its cooling time. The cooling time, t_{syn} is proportional to $(h\nu)^{-1/2}$ as in the case of ES and in agreement with observations. This is a general feature of synchrotron radiation. An observation of this feature can,

therefore, verify that synchrotron radiation takes place in GRBs but it would not distinguish between the ES and the IS scenarios.

Using Eqs. 25 we calculate the duty-cycle D defined as the ratio of the cooling time to the total duration:

$$D \equiv \frac{t_{\text{syn}}}{t_{\text{dur}}} = 1.4 \times 10^{-4} \epsilon_B^{-3/4} \zeta^{3/2} \left(\frac{h \nu_{\text{obs}}}{100 \text{ KeV}} \right)^{-1/2} \times \left(\frac{\gamma}{100} \right)^4 \left(\frac{t_{\text{dur}}}{10 \text{ s}} \right)^{5/4} E_{51}^{-3/4}. \quad (25)$$

The duty cycle increases with burst duration, but it is short enough to explain the high variability even for bursts as long as 100sec. This is different from the ES scenario in which the duty-cycle was only weakly decreasing with burst duration. Since duration changes by about four orders of magnitude it might be possible to distinguish between the two models. Note, however, that in internal shocks the synchrotron cooling is so rapid that another process (such as the acceleration within the shock) could easily be slower and it would determine the shortest observe time scale. Thus, the strong dependence of t_{syn} on t_{dur} might be screened and undetectable.

The cooling time scale increases as the magnetic field decreases. Most GRBs are highly variable with a duty-cycle of order of 5% or less. This sets a lower limit to the value of ϵ_B :

$$\epsilon_B \geq 3.8 \times 10^{-4} \zeta^2 \left(\frac{h \nu_{\text{obs}}}{100 \text{ KeV}} \right)^{-2/3} \times \left(\frac{D}{0.05} \right)^{-4/3} \left(\frac{\gamma}{100} \right)^{16/3} \left(\frac{t_{\text{dur}}}{10 \text{ s}} \right)^{5/3} E_{51}^{-1}. \quad (26)$$

Unlike ES, the magnetic field here can be quite far from equipartition. This eases somewhat the requirement on the processes that build up the magnetic fields in the shocks and it is possible that the magnetic field dragged along the fluid from the source might be sufficient.

6 INVERSE COMPTON SCATTERING

Inverse Compton (IC) scattering may modify our analysis in several ways. IC can influence the spectrum even if the system is optically thin (as it must be) to Compton scattering (see e.g. Rybicki & Lightman, 1979). The effect of IC depends on the Comptonization parameter $Y = \gamma^2 \tau_e$. It can be shown (SNP) that Y satisfies:

$$Y = \epsilon_e / \epsilon_B \quad \text{if} \quad \epsilon_e \ll \epsilon_B \quad (27)$$

$$Y = \sqrt{\epsilon_e / \epsilon_B} \quad \text{if} \quad \epsilon_e \gg \epsilon_B.$$

IC is unimportant if $Y < 1$ and in this cases it can be ignored.

If $Y > 1$, which corresponds to $\epsilon_e > \epsilon_B$ and to $Y = \sqrt{\epsilon_e / \epsilon_B}$ then a large fraction of the low energy synchrotron radiation will be up scattered by IC and a large fraction of the energy will be emitted via the IC processes. If those IC up scattered photons will be in the observed energy band then the observed radiation will be IC and not synchrotron photons. If those IC photons will be too energetic, then IC will not influence the observed spectra but as it will take a significant fraction of the energy of the cooling electrons it will influence the observations in two ways: it will shorten the cooling time (the emitting electrons will be cooled by

both synchrotron and IC process). Second, it will influence the overall energy budget and reduce the efficiency of the production of the observed radiation. We turn now to each of this cases.

Consider, first, the situation in which $Y > 1$ and the IC photons are in the observed range so that some of the observed radiation may be due to IC rather than synchrotron emission. This is an interesting possibility since one might expect that the IC process to ease the requirement of rather large magnetic fields that is imposed by the synchrotron process. We show here that, somewhat surprisingly, this is not the case.

An IC scattering boosts the energy of the photon by a factor γ_e^2 . Therefore, the Lorentz factor of electrons radiating synchrotron photons which are IC scattered on electrons with the same Lorentz factor and have energy $h\nu$ in the observed range is the square root of γ_e given by Eq. 22. These electrons are cooled both by synchrotron and by IC. The latter is more efficient and the cooling is enhanced by the Compton parameter Y . We can now estimate the duty-cycle (the ratio of the cooling time to the overall duration):

$$D = 0.014\epsilon_B^{-3/8}\epsilon_e^{-1/2}\zeta^{7/4}\left(\frac{\gamma}{100}\right)^{9/2} \times \left(\frac{t_{dur}}{10 \text{ sec}}\right)^{13/8} E_{51}^{-7/8} \left(\frac{h\nu_{obs}}{100 \text{ KeV}}\right)^{-1/4}. \quad (28)$$

This duty-cycle depends strongly on the duration, a fact that was not observed. Additionally, it scales with the observed photon's energy as $(h\nu)^{-1/4}$ while observation are more compatible with $(h\nu)^{-1/2}$ (Fenimore *et. al.*, 1995). It is unlikely therefore, that the observed radiation is due to IC process. In addition, inspection of Eq. 28 shows that the magnetic field cannot be very small even in this case. If ϵ_B is too small D will become larger than unity.

Finally, if $Y > 1$ IC will influence the process even if the observed photons are not produced by IC. It will speed up the cooling of the emitting regions and shorten the cooling time, t_{syn} estimated earlier by a factor of Y . With this increase in the cooling rate the duty-cycle limit on the magnetic field become extremely small. However, these very low magnetic field values are impossible since in addition IC also reduces the efficiency by the same factor, and the efficiency becomes extremely low as described below.

The efficiency of a burst depends on three factors: first only the electrons' energy is available. This yields a factor ϵ_e . Second, there is an additional factor of $\sqrt{\epsilon_B/\epsilon_e}$ if the IC radiation is not observed. Third, only the energy radiated by electrons with $\gamma \geq \hat{\gamma}$ is observed, and assuming a a power law electron distribution with an index $\bar{\beta} = -2.5$ (see SNP and the previous section) this gives a factor of $(\gamma_{min}/\hat{\gamma})^{1/2}$. The total efficiency is the multiplication of those three factors and assuming that $\epsilon_B < \epsilon_e$ it is given by:

$$\epsilon_{tot} \geq 0.24\epsilon_B^{5/8}\epsilon_e\zeta^{-1/4}E_{51}^{1/8}\left(\frac{\gamma}{100}\right)^{-1/2}\left(\frac{t_{dur}}{10 \text{ s}}\right)^{-3/8}. \quad (29)$$

The efficiency can be rather high provided that the electrons and the magnetic field energy density are close to equipartition. This efficiency equation sets a stronger lower limit for the magnetic field than the duty-cycle lower. As in the ES case the efficiency increases when the burst duration decreases.

7 DISCUSSION

We have calculated the hydrodynamic and cooling time scales of GRBs produced by internal shocks. We have found that internal shocks could easily explain the observed complicated temporal structure of GRBs: it directly reflects the temporal behavior of the inner engine that drives the GRB. Recall, that this is not the case in the ES scenario (SP). The duration is dictated by Δ , the width of the relativistic shell, which in turn corresponds to the total duration of the emission of the internal source. The duration of individual peaks is determined by δ the length scale over which the conditions in the shell vary significantly. The length δ , is again dictated by the temporal scale of variability of the internal source. This scenario agrees, therefore, with the conclusion of Li & Fenimore (1996) who discovered that the mid-peak intervals has a Log-Normal distribution which indicates a causal relation between peaks and concluded that the temporal structure is driven by the inner source.

The opacity, and in particular the opacity to pair-production poses a sever constraint on the parameter space. The strongest constrain appears if we demand that an observed 100MeV photon can escape freely from the system (Fenimore, Epstein and Ho, 1993; Woods and Loeb, 1995). The fact that there are such observed photons and that EGRET observes even higher energy photons suggests that this demand is reasonable. If the observed spectrum is unbounded than this yields a strong limit and only a narrow strip is allowed for optically thin IS in the γ , δ plane. The most worrisome fact is that there is no single value of γ (or δ) which can account for all kinds of observed bursts and the shape of this allowed region demands a correlation (in fact anti-correlation) between γ and δ . This is not impossible but it seems unlikely. Alternatively this suggests that bursts with short peaks will be optically thick to 100MeV photons and such photons won't be observed in those bursts.

If there is an upper cutoff E_{max} to the observed spectrum then the optically thickness problem is weaker and pair-production simply set a limit of a minimal Lorentz factor of $\sim E_{max}/2m_e c^2$ which is $\gamma \approx 100$ for 100MeV photons. Even in this case the optical depth to Compton scattering becomes larger than unity for small values of δ - which correspond to very short peaks. The allowed region is wider but once more either there is some correlation between γ and δ or we should observe optically thick narrow peak bursts.

Like in the ES scenario the radiation process is most likely synchrotron. In spite of the higher energy density in the internal shock region (higher compared to the densities in the ES scenario) the magnetic field values required are, close to the equipartition value. Otherwise, the efficiency will become too low! Inverse Compton (IC) is possible - but quite unlikely. Somewhat surprisingly IC cooling requires magnetic fields that are as high as those required for synchrotron cooling. Again if these values are too small then efficiency constraints will rule out the model.

Synchrotron cooling in the IC scenario suggests a correlation between the cooling time and the overall duration: $t_{syn} \propto t_{dur}^{9/4}$. This is a high power and if t_{syn} determines the duration of the shortest peaks it might be observed since t_{dur} varies by four orders of magnitude. This should be compared to the cooling time in the ES scenario which varies like $t_{dur}^{3/4}$. However, the cooling rate in the IS scenario is so rapid that

this possible correlation may be masked by another process, e.g. the acceleration within the shocks, that would be slower and would determine the duration of the shortest peaks.

ACKNOWLEDGMENTS

We thank Ramesh Narayan and Jonathan Katz for helpful discussions. This research was supported by the US-Israel BSF science foundation and by the Israel NSF.

REFERENCES

Fenimore, E., E., Epstein, R., I., & Ho, C., 1993, A&A Supp. **97**, 59.

Fenimore, E. E., *et. al.*, 1995, ApJL, **448**, L101.

Fenimore, E. E., Madras, C. D., & Nayakshin, S., 1996, ApJ, in press, astro-ph/9607163.

Fishman, G. J., & Meegan, C. A., 1995, Ann. Rev. A&A, **33**, 415.

Goodman, J. 1986, ApJ, 308, L47.

Katz, J., I., 1994, ApJ, **432** L107-109.

Krolik, J. H., & Pier, E. A. 1991, ApJ, 373, 277.

Li, H. & Fenimore, E., E., 1996, ApJ. Lett, in press, astro-ph/9607131.

Mészáros, P. & Rees, M. J., 1992. **258**, 41p.

Narayan, R., Paczyński, B., & Piran, T. 1992, ApJ, **395**, L83.

Narayan, R., & Piran, T. 1994, unpublished.

Paczyński, B. 1986, ApJ, 308, L51.

Piran, T. 1994, in AIP Conference Proceedings 307, Gamma-Ray Bursts, Second Workshop, Huntsville, Alabama, 1993, eds. G. J. Fishman, J. J. Brainerd, & K. Hurley (New York: AIP), p. 495.

Piran, T., 1996 astro-ph/9507114 to appear in *Some unsolved problems in Astrophysics* Eds. Bahcall, J. and Ostriker, J. P. Princeton University Press.

Rees, M. J., & Mészáros, P. 1994, ApJ, 430, L93.

Rybicki, G. B. & Lightman, A. P., 1979, "Radiative Processes in Astrophysics", Willy-Interscience, New York.

Sari, R., & Piran, T., 1995, ApJ, **455** L143 (denoted SP).

Sari, R., & Piran, T., 1996, in preparation.

Sari, R., Narayan, R. & Piran, T., 1995, ApJ, in press (denoted SNP).

Shaviv, N., & Dar, A., 1995, Mon. Not. R. astr. Soc., **277**, 287.

Shaviv, N., & Dar, A., 1996, astro-ph/9606032.

Woods, E. & Loeb, A., 1995, ApJ, **453**, 583.